

HFORD: High-Fidelity and Occlusion-Robust De-identification for Face Privacy Protection

Dongxin Chen, Mingrui Zhu, Nannan Wang, *Member, IEEE*, and Xinbo Gao, *Senior Member, IEEE*

Abstract—With the popularity of smart devices and the development of computer vision technology, concerns about face privacy protection are growing. The face de-identification technique is a practical way to solve the identity protection problem. The existing facial de-identification methods have revealed several problems, including the impact on the realism of anonymized results when faced with occlusions and the inability to maintain identity-irrelevant details in anonymized results. We present a High-Fidelity and Occlusion-Robust De-identification (HFORD) method to deal with these issues. This approach can disentangle identities and attributes while preserving image-specific details such as background, facial features (e.g., wrinkles), and lighting, even in occluded scenes. To disentangle the latent codes in the GAN inversion space, we introduce an Identity Disentanglement Module (IDM). This module selects the latent codes that are closely related to the identity. It further separates the latent codes into identity-related codes and attribute-related codes, enabling the network to preserve attributes while only modifying the identity. To ensure the preservation of image details and enhance the network’s robustness to occlusions, we propose an Attribute Retention Module (ARM). This module adaptively preserves identity-irrelevant details and facial occlusions and blends them into the generated results in a modulated manner. Extensive experiments show that our method has higher quality, better detail fidelity, and stronger occlusion robustness than other face de-identification methods.

Index Terms—Privacy protection, face de-identification, identity disentanglement, occlusion robustness.

I. INTRODUCTION

WITH the widespread use of smart devices and the rapid development of Computer Vision (CV), there are many ways to obtain facial images. For example, individuals can obtain them by taking photos using smart devices or compositing photos using CV technology. If attackers illegally obtain identity information, they might use CV technology to synthesize forged face images of the same identity. Since facial identity is critical in security and payments, protecting identity information is significant. Face de-identification technology produces anonymized images to hide identities, thereby successfully alleviating identity protection issues. Initially, face de-identification operated on identity information at the pixel level, including noise, blur, and masking. Although these methods effectively protect identity information, they reduce image quality and practicality [1].

GAN-driven techniques [2]–[4] have previously produced significant enhancements to face de-identification. These methods successfully generate face images with the same attributes but different identities, thus promoting significant progress in anonymity protection. However, the results still show artifacts,

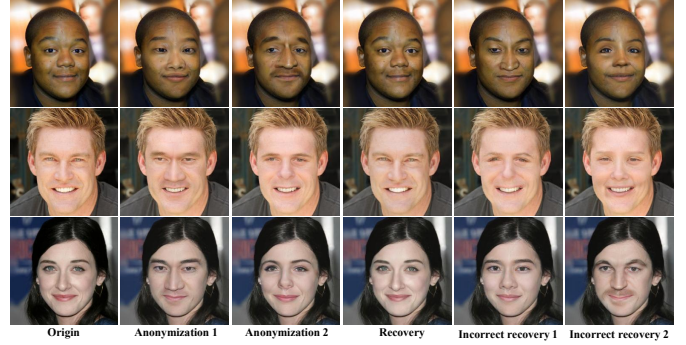


Fig. 1. Our de-identification and recovery results in the wild. The first column shows the faces to be protected. The second and third columns show the anonymous faces generated by different passwords. The fourth column shows the faces recovered by the correct passwords. The fifth and sixth columns show the faces recovered by incorrect passwords.

making the fakeness of the image obvious. At the same time, many methods neglect to preserve the attribute details in the source image (such as background and brightness), which leads to apparent differences between the attributes of the generated results and the original attributes.

Most previous methods only focus on anonymity and ignore the importance of recovering the initial identity. In cases involving legal matters or relatives, individuals preferred original images over anonymous ones. Therefore, reversibility must be considered in the de-identification process.

In recent years, reversible de-identification techniques have emerged. FIT [5] achieves anonymity through essential networks and complex loss functions, which hinders its improvement in generation quality and robustness. Personal [6] proposes tailor-made manual encryption rules to achieve anonymity, compromising the network’s flexibility and security. RiDDLE [7] proposes a clear anonymization strategy, which can produce higher-quality generation results. However, due to the distortion problem of StyleGAN [8], [9], RiDDLE [7] achieves attribute preservation with the assistance of the face parsing model, which makes it ineffective in memorable scenes such as occlusion.

A face de-identification method should have the following characteristics: (1) Generate diverse and realistic de-identified faces. (2) Reliably recover the original identity. (3) Generate new identities to protect privacy in insecure situations. (4) Preserve identity-irrelevant details while generating high-quality anonymous faces. (5) Generate high-quality anonymous results in the face of occlusion.

Specifically, we propose a High-Fidelity and Occlusion-

Robust De-identification (HFORD) method, which has strong robustness and high generation quality. To disentangle the latent codes in the W latent space, we propose an Identity Disentanglement Module (IDM), which effectively separates latent codes into identity-related codes and attribute-related codes, enabling the network to preserve attributes while only modifying the identities. Furthermore, to ensure the preservation of image details and enhance the network’s robustness to occlusions, we propose an Attribute Retention Module (ARM). It adaptively preserves identity-independent details and facial occlusions and blends them into the generated results in a modulated manner. Compared with previous work, our approach not only achieves reversible de-identification but also generates de-identification results with higher fidelity and naturalness, as well as the ability to handle occlusion issues. Fig. 1 shows the de-identification and recovery results.

In summary, our main contributions are as follows:

- We propose a hierarchical de-identification method HFORD that enables high-fidelity and occlusion-robust de-identification in the W latent space.
- We design an IDM in W latent space that enables it to select identity-related latent codes dynamically and skillfully disentangle identities and attributes.
- We propose an ARM to solve the distortion problem of StyleGAN. This innovative approach not only preserves the intricate details of the source image but also produces robust results against occlusions.
- Experimental results show that our approach outperforms previous work regarding de-identification and recovery quality, detail fidelity, and occlusion robustness on public datasets.

II. RELATED WORK

A. Face De-identification

Face de-identification involves changing or hiding the identity in facial images to protect personal privacy from attackers. Traditional techniques for facial de-identification include blurring, masking, introducing noise, and applying pixelation. Although they effectively protect face identities, these methods significantly impact image fidelity, which weakens their usefulness.

Due to the advancement of Generative Adversarial Networks (GANs), face de-identification mainly relies on GANs to generate higher-quality de-identified images. Recently, attention to facial de-identification has increasingly revolved around changing a person’s identity while preserving identity-independent attributes. Some work [4], [10], [11] optimize network or latent code for de-identification by minimizing the cosine similarity of identity features. Gafni et al. [4] proposed a multi-level perceptual loss for de-identification by minimizing overall differences at lower levels and maximizing fine-grained differences at higher levels. Wu et al. [10] generated anonymous images by maximizing identity feature differences. Barattin et al. [11] believe that layers 3-7 of latent codes in W latent space are related to face identity, and they optimize the latent codes of these layers to achieve anonymization under specific loss constraints. The optimization method makes the

inference time longer and affects its practicality. This method does not explicitly disentangle identities and attributes. The generated results may contain part of the previous identity information. Other works [2], [3], [12]–[14] hide facial regions and synthesize new faces using provided attribute information. DeepPrivacy [2] conditionally generates anonymous images that satisfy the facial surroundings and sparse pose information. CIAGAN [3] expects to control the generated anonymous identities via landmarks, masks, and desired identities. Although the above works can generate anonymous faces, they often suffer from unnaturalness, lack of diversity, and poor practicality.

Recently, reversible face de-identification technology [5]–[7] has attracted attention. FIT [5] uses predefined binary passwords and face images to train a generative adversarial network, which can achieve anonymity through passwords and recover the original face through inverse passwords. Personal [6] disentangles the input image in the feature space and changes the identity features through customized mathematical formulas to achieve anonymization and recovery. RiDDLE [7] maps the image to W latent space through GAN inversion, and the password acts as information for other modalities, guiding the editing of the latent code to change the identity. These methods use customized encryption strategies or flawed modules that may affect the origin identity’s security and the resulting images’ quality. Redundant processing also results in reduced robustness of de-identification. Different from the above methods, our approach is more robust and secure.

B. Face Identity Disentanglement

Face identity disentanglement focuses on separating the identity representation and attribute representation in face images to achieve the preservation or editing of face identity. Most identity-related disentanglement tasks use pre-trained face recognition networks to extract identity features to guide network training. In the face-swapping task, Bao et al. [15] designed a simple disentangled network trained using an asymmetric loss to separate identity from attributes. Li et al. [16] proposed a novel generator to modulate the disentangled identity and attribute representations adaptively. Nitzan et al. [17] designed a disentanglement framework based on StyleGAN, where face identity and attributes are disentangled in Z feature space. Luo et al. [18] proposed a new disentanglement framework based on StyleGAN, where an adaptive attribute extractor preserves identity-irrelevant features. In addition to the proposed disentanglement framework, Na [19] introduced 3D spatial representation to improve the completeness of attribute representation. In the facial identity preservation task, Shen et al. [20] suggest considering a facial identity classifier as a third player in the game to facilitate the disentanglement of identities and attributes. Shoshan et al. [21] used contrastive learning to obtain a GAN with an explicit disentangled latent space. Li et al. [16] designed a region discovery module to locate identity-irrelevant attributes of faces to generate privacy-preserving faces adaptively. In the face de-identification task, Ma et al. [22] used spherical spatial units to represent disentangled identities and edited the identities by changing angles.

Le et al. [23] selected three latent layers most relevant to the identity in W latent space and transformed the identities by changing the latent codes in the selected layers. Jeong et al. [24] applied the manifold k-same algorithm to the disentangled identity representation to achieve de-identification.

C. GAN Inversion

GAN inversion maps an image into a disentangled latent space, enabling manipulation of its identity. Several GAN inversion techniques are currently available. Notably, StyleGAN [8], [9] stands out for its high resolution and realistic generated results, making it the first choice for most inversions involved. An optimization-driven approach [25]–[27] treats latent codes as an object of optimization. These methods iteratively refine the latent code by imposing loss constraints aligning the generated output with the desired goal. While such methods tend to exhibit excellent reconstruction and editing results, they are more time-consuming and resource-intensive during inference. Encoder-based techniques [28]–[30] utilize a specially designed encoder to map the input image to the W latent space. This method has a simplified inference process, but the fidelity is reduced compared to optimization-driven methods. Given the trade-off between result fidelity and generation efficiency, we choose an encoder-based inversion approach [30].

III. APPROACH

A. Preliminaries

Given the face images to be protected, our goal is to design a network that can generate anonymized images and images with the original identity from the anonymized image. The original image X^{ori} , the anonymous image X^{anony} , and the recovered images X^{re} are respectively defined as $X^{ori} \in \{X_1^{ori}, X_2^{ori}, X_3^{ori}, \dots\}$, $X^{anony} \in \{X_1^{anony}, X_2^{anony}, X_3^{anony}, \dots\}$, $X^{re} \in \{X_1^{re}, X_2^{re}, X_3^{re}, \dots\}$. The attribute information of X^{anony} is consistent with X^{ori} , such as background and expression. In contrast, identity-related information is modified, such as eyes and nose. The users must set a password P for anonymity and identity recovery. During the anonymous phase, the user sets a password P for anonymity. Different passwords can produce different anonymous results. In the recovery phase, when P is the correct password, the network generates a face image X^{re} with the same attributes and identity as the original image. When P differs from the correct password, the network generates the face images with the same attributes as the original images but with different identities. The result of wrong recovery X^{wr} can be defined as $X^{wr} \in \{X_1^{wr}, X_2^{wr}, X_3^{wr}, \dots\}$. Fig. 2 illustrates the process of the proposed method.

B. Overall Architecture

Our framework HFORD contains an e4e encoder [30], an IDM, an ARM, a pre-trained StyleGAN2 generator [9], and three conditional MLP (cMLP). Fig. 3 shows the de-identification framework with reversible high-fidelity and occlusion robustness. In the anonymity stage, the input is the face

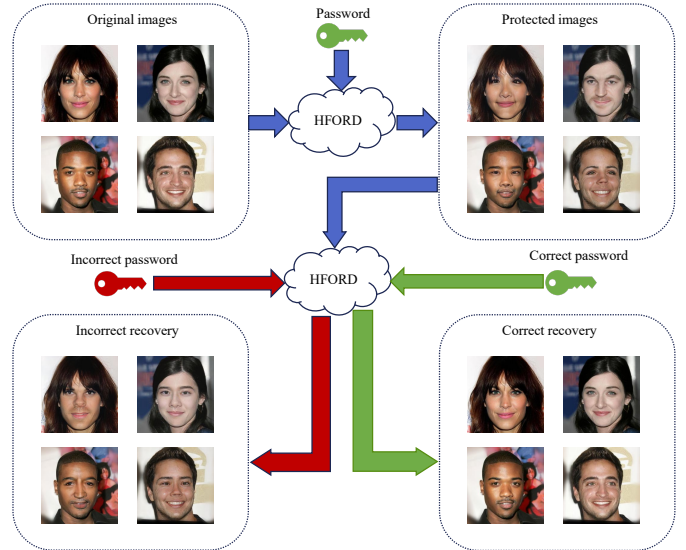


Fig. 2. Illustration of the proposed framework. In the anonymization phase, the user sets a personalized password. In the recovery phase, when the entered password is the same as that set during the anonymity phase, the network generates an image with the correct identity. If the password is inconsistent with the one set during the anonymity phase, the network will generate an image with an incorrect identity to protect the user’s privacy.

images X^{ori} to be protected. The latent code C is obtained after GAN inversion. The latent code C is split into three sub-latent codes for more granular identity modification. The latent code can be expressed as $C = \{C^c, C^m, C^f\}$, and its superscripts c, m, and f represent coarse, medium, and fine, respectively. The division rules of c, m, and f refer to RiDDLE [7]. To disentangle the identity information and attribute information, we elaborately design an IDM with a ViT-based architecture [31] to split the latent code C into the identity latent code I and the attribute latent code A in the W latent space. The identity latent code I , attribute latent code A and password P can be expressed as $I = \{I^c, I^m, I^f\}$, $A = \{A^c, A^m, A^f\}$ and $P = \{P^c, P^m, P^f\}$ respectively. Then, the identity code I and the password P are hierarchically input into the cMLP, and the output of the cMLP is new identity latent code \hat{I} . The new identity latent code \hat{I} can be expressed as $\hat{I} = \{\hat{I}^c, \hat{I}^m, \hat{I}^f\}$. The new identity latent code \hat{I} is element-wise summed with the attribute latent code A to obtain the complete anonymous latent code \hat{C} , which can be expressed as $\hat{C} = \{\hat{C}^c, \hat{C}^m, \hat{C}^f\}$. The anonymous latent code \hat{C} is hierarchically input into StyleGAN to complete the anonymization process. To solve the distortion problem of StyleGAN, we propose a multi-scale ARM based on the attention mechanism. The feature map M obtained from e4e is rich in attribute information but contains other redundant information. It is also divided into three levels, and the feature map sizes of c, m, and f correspond to 16, 32, and 64, respectively. M can be expressed as $M = \{M^c, M^m, M^f\}$. The feature maps M are input into the ARM, and the output of ARM \hat{M} is the detailed information ignored by StyleGAN. \hat{M} can be expressed as $\hat{M} = \{\hat{M}^c, \hat{M}^m, \hat{M}^f\}$. Finally, the details \hat{M} are fused with the complete anonymized latent code \hat{C} in

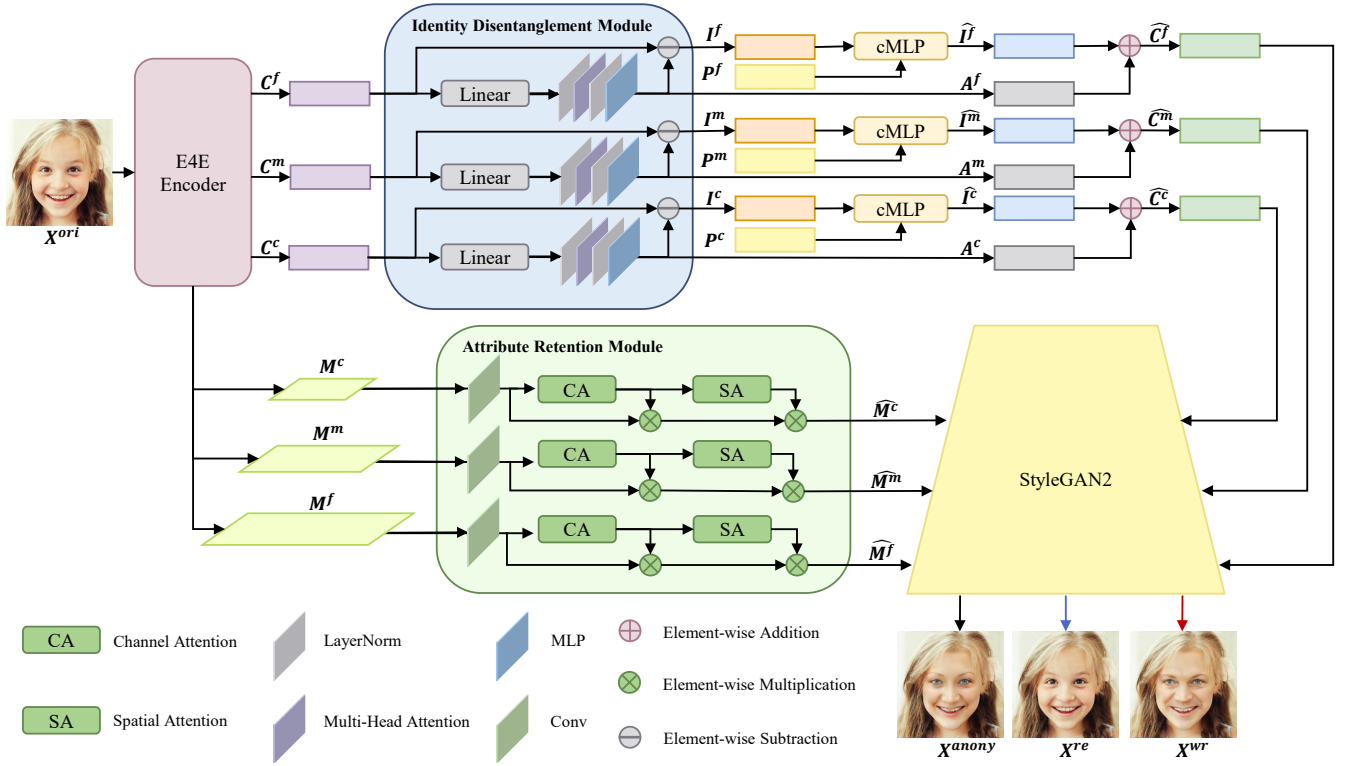


Fig. 3. Our proposed overall architecture for de-identification. The network consists of a GAN inversion encoder, an IDM, an ARM, a StyleGAN generator, and three cMLP at different scales. The user sets a personalized password during the anonymization process, and the black arrow points to the anonymous result. During the recovery process, if the password is consistent with the anonymous one, the network outputs the correct recovery result, as shown in the image pointed by the blue arrow. If the password is different from the anonymous one, the network will output incorrect recovery results, as in the image pointed by the red arrow.

StyleGAN to generate the anonymized image X^{anony} . In the recovery phase, the new identity latent code \hat{I} and password P are used as input to obtain the recovered image X^{re} , and the rest of the process is consistent with anonymity.

C. Identity Disentanglement Module

We propose an IDM, as shown in Fig. 3. Different levels of latent codes correspond to different disentangled layers. We divide the disentangled layers into coarse disentangled layers, medium disentangled layers, and fine disentangled layers. The multi-head attention mechanism mentioned in Transformer [32] divides the model into multiple subspaces, allowing the model to focus on the required information. We utilize a multi-head attention mechanism to select attribute information in coarse, medium, and fine layers. The following equation can express the multi-head attention mechanism,

$$MultiHead(Q, K, V) = \text{Concat}(\text{head}_1, \dots, \text{head}_h)W^O, \quad (1)$$

$$\text{head}_i = \text{softmax}\left(\frac{QW_i^Q(KW_i^K)^T}{\sqrt{d_k}}\right)VW_i^V, \quad (2)$$

where the projections are parameter matrices $W_i^Q \in \mathbb{R}^{d_{model} \times d_k}$, $W_i^K \in \mathbb{R}^{d_{model} \times d_k}$, $W_i^V \in \mathbb{R}^{d_{model} \times d_v}$ and $W^O \in \mathbb{R}^{hd_v \times d_{model}}$, d_k is the scaling factor, and h is heads.

Based on the ViT architecture [31], IDM links attribute information between different locations through multi-head

attention and separates entangled identity codes I from attribute codes A under loss constraints. First, the e4e encoder takes the face images X^{ori} as input to generate the latent code C . According to RiDDLE's [7] customized layering rules, the coarse layer is 1-4 layers, the medium layer is 5-8, and the fine layer is 9-14. The specified latent codes are input into the IDM of the corresponding scale respectively to obtain the attribute latent codes A . Since the W latent space has linearity [8], we regard the difference between C and A as I .

D. Attribute Retention Module

We apply Spatial Attention (SA) and Channel Attention (CA) mechanisms to ARM. The SA focuses on the most meaningful features in space, which can be expressed by the following equation,

$$SA(M) = \sigma(\text{Conv}(\text{MaxPool}(M) \oplus \text{AvgPool}(M))), \quad (3)$$

where σ is the sigmoid activation function and \oplus is the concatenate operation.

Redundant channel information affects the network. The CA can ignore redundant channel information and make the network pay more attention to valuable channels. The following equation can express CA,

$$CA(M) = \sigma(\text{MLP}(\text{AvgPool}(M)) + \text{MLP}(\text{MaxPool}(M))). \quad (4)$$

Due to the limitations of StyleGAN, rich attribute information is represented by low-dimensional latent codes, resulting in lower fidelity of generated results. We propose an attention-based multi-scale ARM to preserve attributes such as face details and background. It selects attribute-related information in the feature map provided by the e4e encoder through the SA and CA mechanisms and generates feature map \widehat{M} containing only attributes. \widehat{M} is one of the inputs to StyleGAN and is used to compensate for the missing attribute information of W in the latent code. The following equation can express the process of ARM,

$$\begin{aligned} ARM(M) = SA(CA(Conv(M))) \\ \cdot (Conv(M) \cdot CA(Conv(M))). \end{aligned} \quad (5)$$

E. Loss Functions

Pre-training without cMLP is performed before anonymity training to facilitate identity and attribute disentanglement. At the same time, since it does not contain L_{id} , the model converges faster than during anonymous training. See III-F for the specific pre-training process. X^{attr} is defined as an image providing attributes, and X^{id} is defined as an image providing identity. We use X^{attr} to provide the multi-scale feature map M and attribute latent code A , and X^{attr} provides the identity latent code I . The output X^{mix} is defined as an image with the identity of X^{id} and the attributes of X^{attr} . At the same time, we designed a special contrast loss only for the pre-training process. Its formula is as follows,

$$L_c = \begin{cases} \max(d(X^{mix}, X^{attr}) - \tau^+, 0) & X^{id} = X^{attr}, \\ \max(\tau^- - d(X^{mix}, X^{attr}), 0) & otherwise. \end{cases} \quad (6)$$

where τ^+ is the threshold when the identity image X^{id} is equal to the attribute image X^{attr} . τ^- is the threshold when the identity image X^{id} is different from the attribute image X^{attr} . d is the distance function of the identity feature, denoted as

$$d(X^{mix}, X^{attr}) = 1 - \cos(F_a(X^{mix}), F_a(X^{attr})), \quad (7)$$

where \cos indicates cosine similarity. F_a is pre-trained ArcFace [33], used to extract identity features.

To assist the ARM in learning the details of the image, we apply LPIPS loss [34] to the generated images $X^* \in \{X^{anony}, X^{re}, X^{wr}, X^{mix}\}$, to maintain the image quality and the consistency of low-level attribute features, denoted as

$$L_{lips} = \|F_l(X^{ori}) - F_l(X^*)\|_2, \quad (8)$$

where F_l denotes the pre-trained perceptual feature extractor and X^* denotes all generated faces.

We use L_1 reconstruction loss to keep the overall structure similar, with the following equation,

$$L_{rec} = \|X^{ori} - X^*\|_1. \quad (9)$$

To induce differences in passwords to cause high-level identity changes, we define identity difference loss, denoted as

$$L_{dif} = \frac{1}{n(n-1)} \cdot \sum_{\substack{x_i, x_j \in X \\ i \neq j}} \max(0, \cos(F_a(x_i), F_a(x_j))), \quad (10)$$

where X is equal to the union of the de-identified face X^{anony} and the incorrectly recovered face X^{wr} , which can be expressed as $X = \{X^{anony}, X^{wr}\}$. The variable n denotes the number of elements of the set X .

To hide the identity of the face, we design the anonymization loss so that the distance between the identity features of the generated face and the identity features of the original face is greater than the threshold of the face recognition model, denoted as

$$L_{anony} = \frac{1}{n} \cdot \sum_{x_i \in X} \max(0, \cos(F_a(X^{ori}), F_a(x_i))), \quad (11)$$

where X^{ori} is the face to be protected.

As reversible face de-identification, the network can recover the original face. We constrain the cosine distance of the identity features between the correct recovery face and the original face to achieve reversibility, denoted as

$$L_{rev} = \frac{1}{m} \cdot \sum_{x_z \in X^{re}} (1 - \cos(F_a(X^{ori}), F_a(x_z))), \quad (12)$$

X^{re} denotes the correctly recovered face, and m denotes the number of elements in X^{re} .

The total identity loss can be expressed as

$$L_{id} = L_{dif} + L_{anony} + L_{rev}. \quad (13)$$

The anonymity direction is uncontrollable, and the generated faces may have unnatural features. To make the generated face shape natural, we apply a face parsing loss,

$$L_{parse} = \|F_p(X^{ori}) - F_p(X^*)\|_2, \quad (14)$$

where F_p denotes the pre-trained face parsing model from [36]. We only choose identity-related parts for loss.

To make the output latent code w close to the W^+ latent space, we define the following regularization loss,

$$L_{reg} = \sum_{i=1}^{N-1} \|\Delta_i\|_2, \quad (15)$$

where w denotes the style code of all output latent codes, and Δ denotes a set of offsets based on w . The constant N indicates the number of latent code layers.

We use adversarial loss with R_1 regularization [37] to improve the realism of the generated faces, with the same discriminator construct as in StyleGAN2 [9], calculated as follows,

$$\begin{aligned} L_{adv}^D = -\mathbb{E}[\log D(X^{ori})] - \mathbb{E}[\log(1 - D(X^*))] \\ + \frac{\gamma}{2} \mathbb{E}[\|\nabla D(X^{ori})\|_2^2], \end{aligned} \quad (16)$$

$$L_{adv}^G = -\mathbb{E}[\log D(X^*)]. \quad (17)$$

The total loss function can be expressed as

$$\begin{aligned} L_{total} = \lambda_c L_c + \lambda_{id} L_{id} + \lambda_{lips} L_{lips} \\ + \lambda_{rec} L_{rec} + \lambda_{parse} L_{parse} + \lambda_{reg} L_{reg} + L_{adv}. \end{aligned} \quad (18)$$

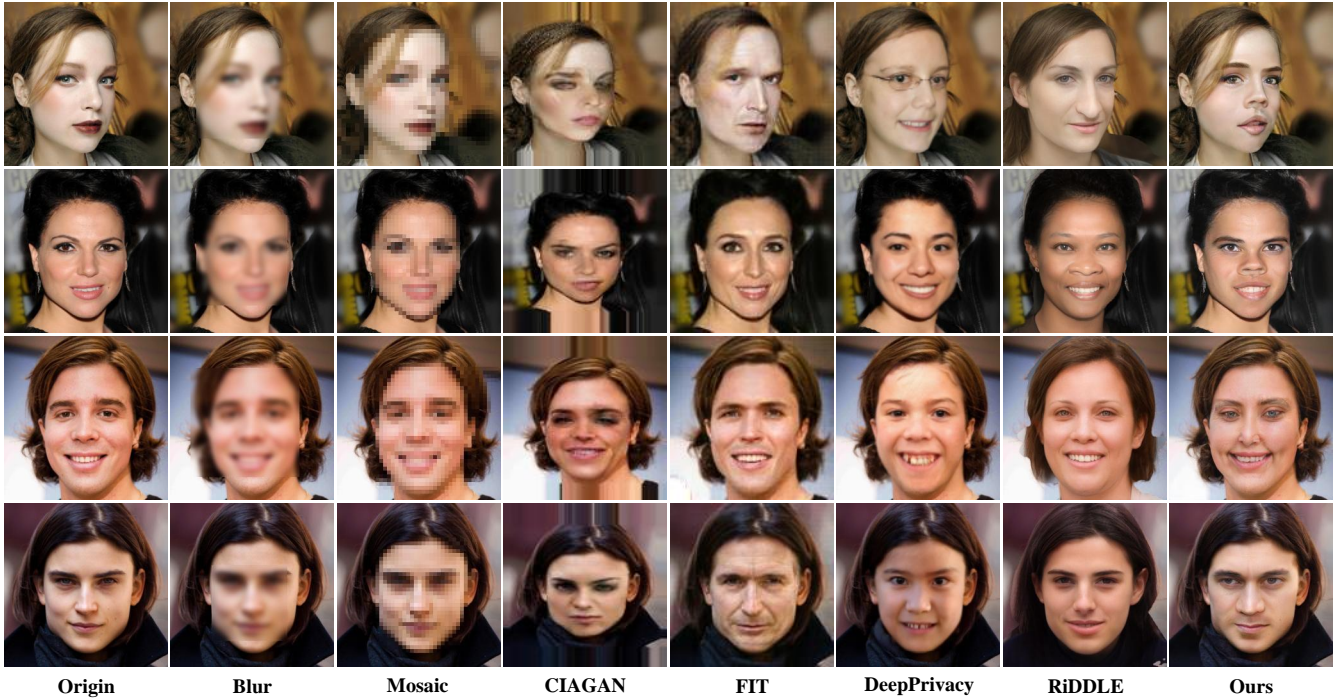


Fig. 4. Compared with existing methods on the CelebA-HQ [35] dataset, our method generates high-quality images while better-maintaining attribute features such as background and wrinkles.

F. Training acceleration strategy

To make the network more focused on anonymity during training, we use a concise loss to pre-train the network before formal training. This strategy enables the network to have a certain degree of disentanglement before starting training and achieve convergence faster. The process is shown in Fig. 5. The pre-trained network does not contain cMLP. At this time, the value of X^{ori} in the loss is taken as X^{attr} .

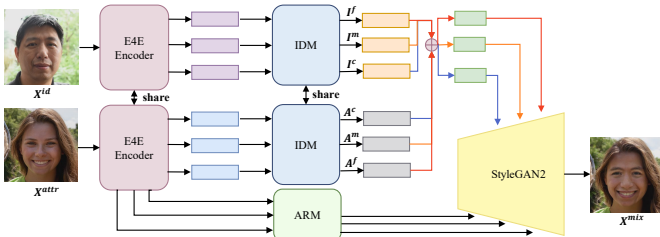


Fig. 5. Network for pre-training process.

The loss does not include L_{id} and uses L_c . The loss is the same as Eq. (18), and the hyperparameters are set to $\lambda_c = 1.0$, $\lambda_{id} = 0$, $\lambda_{lips} = 1.0$, $\lambda_{rec} = 3.5$, $\lambda_{parse} = 0.1$, $\lambda_{reg} = 0.1$.

IV. EXPERIMENTS

A. Experimental Settings

Basic Settings. The network was trained on an NVIDIA Quadro RTX 8000 with a total batch size of 8. We used a Ranger optimizer with a learning rate of 0.0001 for training. The loss is the same as Eq. (18). The hyperparameters of the anonymous training phase are set to $\lambda_c = 0$, $\lambda_{id} = 2.0$,

$\lambda_{lips} = 1.0$, $\lambda_{rec} = 0.05$, $\lambda_{parse} = 0.1$, $\lambda_{reg} = 0.1$. The number of passwords in the anonymization process is 2, one of which is the correct password, and the other is a random password. The number of passwords during the recovery process is 3, including one correct and two incorrect passwords. Therefore, the value of n is 4, and the value of m is 1.

Datasets. We train the network using the FFHQ [8] dataset, which contains 70k high-quality face images. We randomly select 69K images for training and use the remaining images for testing. At the same time, we apply our network to the CelebA-HQ [35] dataset to test the generality of the network. For comparison with similar tasks, we use 256 resolution.

TABLE I

COMPARISON OF IDENTIFICATION RATE WITH OTHER METHODS. THE LOWER THE DE-ID IN THE TABLE, THE BETTER THE PRIVACY PROTECTION. THE HIGHER THE RECOVERY, THE BETTER THE RECOVERY QUALITY. ACCORDING TO [38], THE THRESHOLD OF FACE NET IS $\tau_{facenet} = 1.1$. ACCORDING TO [39], THE THRESHOLD OF ARCFACE IS $\tau_{arcface} = 0.8$. AS SHOWN IN THE TABLE ABOVE, OUR METHOD ACHIEVES THE BEST RESULTS. THE BEST RESULTS ARE SHOWN IN **BOLD**, AND THE SECOND BEST RESULTS ARE MARKED WITH AN UNDERLINE.

	Method	FaceNet (CASIA)	FaceNet (VGGFace2)	ArcFace
De-id↓	CIAGAN [3]	0.120	0.120	0.000
	FIT [5]	0.030	<u>0.055</u>	0.040
	RiDDLE [7]	0.030	0.020	0.005
	DeepPrivacy [2]	<u>0.100</u>	0.095	0.000
	Ours	0.020	0.020	0.000
Recovery↑	FIT [5]	1.000	1.000	1.000
	RiDDLE [7]	0.990	0.995	0.600
	Ours	1.000	1.000	1.000

B. De-identification

As shown in Fig. 4, compared with existing anonymization methods, our method can preserve the details of the original face and produce more realistic results. Since the method Personal [6] is not open source, we use the latest method RiDDLE [7] for comparison. Blurring and mosaic hide the identities but compromise the usefulness of the image, making it easy for attackers to discover that the image has been de-identified. FIT [5] can successfully generate anonymous images with high concealment, but the visual quality of the images is lacking. CIAGAN [3] appears to suffer from unsatisfactory artifacts and severely destroys the original structure of the image. DeepPrivacy [2] has better image quality and realism but generates similar facial features, thus limiting identity diversity. RiDDLE [7] tends to generate diverse and realistic anonymous faces. However, StyleGAN suffers from distortion issues such as losing background and facial details. The face parsing model [36] can help solve the distortion problem, but extracting the background and pasting it behind the face affects the naturalness of the face. Unlike the above methods, our method generates anonymous images with higher fidelity and realism without additional processing.

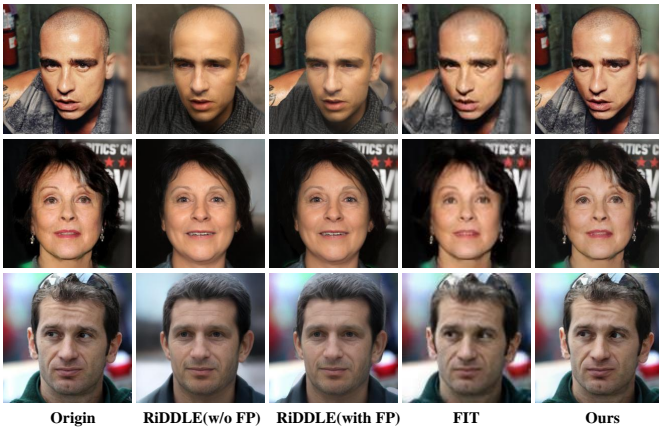


Fig. 6. The results of identity recovery. Our method has high fidelity even at low resolution. FP denotes the face parsing model.

Since neither RiDDLE [7] nor Personal [6] mentions the setting of the de-identification qualitative experiment, to make a fair comparison, we use the same data size and objects to measure the de-identification effect, which may lead to differences with the data in the original paper. We randomly selected $N = 200$ images from CelebA-HQ and anonymized them using a deep learning-based de-identification method. The comparison object for de-identification is the original image, not the reconstructed image generated by StyleGAN (the comparison object of RiDDLE is the reconstructed image). Table I shows the de-identification evaluation results. The results show that our method and RiDDLE [7] can better protect privacy than other methods. Meanwhile, the qualitative results in Fig. 4 show that we can achieve higher fidelity and naturalness than RiDDLE.



Fig. 7. Comparison of the recovery quality on the FFHQ test set. Our approach achieves the best visualization compared to FIT [5] and RiDDLE [7].

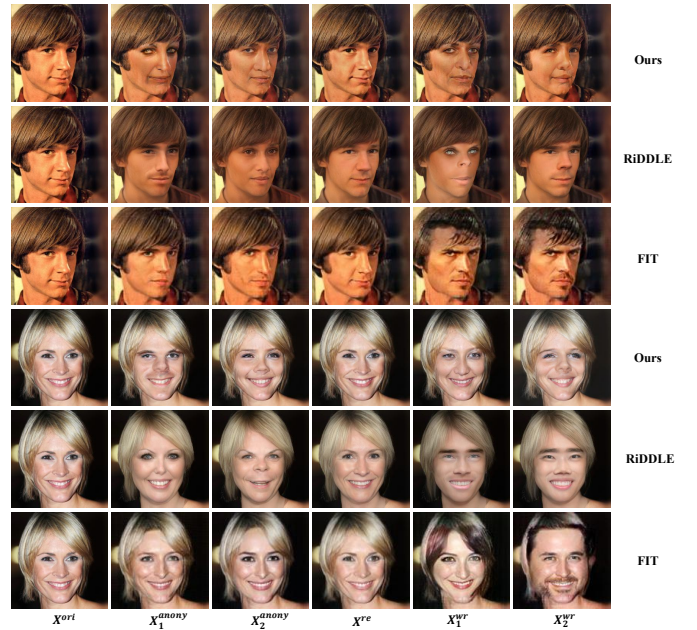


Fig. 8. Generalizability test of the method on CelebA-HQ. Our approach achieves the best visualization compared to FIT [5] and RiDDLE [7].

C. Recovery

We compare our method with the de-identification methods FIT [5] and RiDDLE [7], which have reversible properties. As shown in Fig. 6, our recovery results exhibit higher accuracy and realism. This more vital recovery ability is reflected in the retention of complex details, which is attributed to IDM’s powerful disentanglement ability and ARM’s powerful detail preservation ability. We utilize an attention mechanism to preserve detailed information to achieve high fidelity. Different passwords correspond to different recovery results, as shown

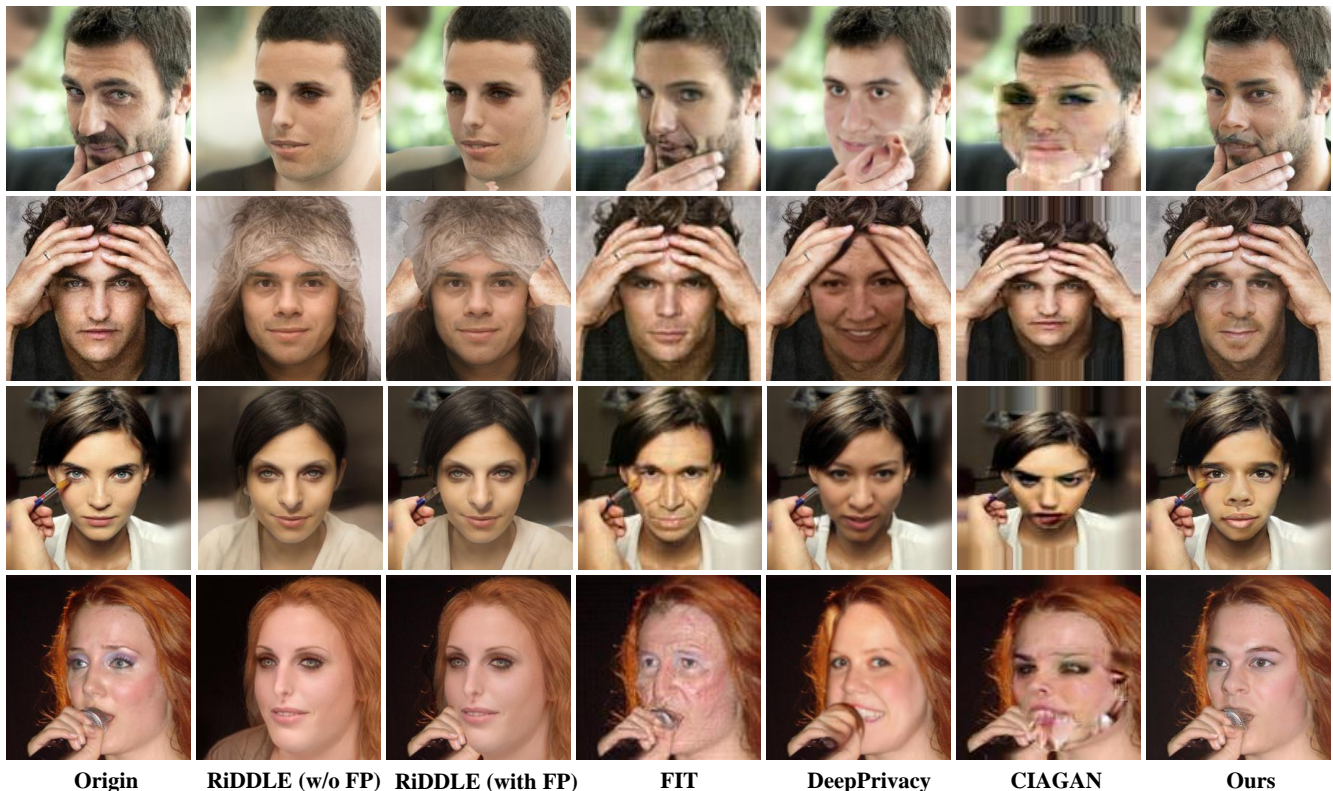


Fig. 9. Anonymous results in special cases. In the case of facial occlusion, our method achieves satisfactory anonymity quality while preserving the original occlusion. FP denotes the face parsing model.

TABLE II
COMPARISON OF RECOVERY QUALITY WITH EXISTING METHODS. THE BEST RESULTS ARE SHOWN IN **BOLD**, AND THE SECOND BEST RESULTS ARE MARKED WITH AN UNDERLINE.

	MSE↓	LPIPS↓	SSIM↑	PSNR↑
FIT [5]	0.006	<u>0.055</u>	0.742	<u>28.275</u>
RiDDLE [7]	0.046	0.188	0.507	19.632
Ours	0.004	0.027	0.819	29.535

in Fig. 7. As the attacker worked to obtain the correct identity, they obtained exquisitely anonymous images due to incorrect password entries. This mechanism effectively protects privacy. We also conducted qualitative experiments on the CelebA-HQ dataset to verify its generalization. As shown in Fig. 8, our method has the highest fidelity and the best recovery.

The setting of the qualitative experiment is consistent with that in IV-B. The results of the recovery recognition rate are shown at the bottom of Table I. To evaluate the similarity of the recovered image to the original image, we used the Learned Perceptual Image Patch Similarity (LPIPS) [34] distance to measure perceptual similarity, the Peak Signal-to-Noise Ratio (PSNR) and the Mean Square Error (MSE) to measure the pixel-level distortion. Structural Similarity (SSIM) measures structural similarity. The results are shown in Table II. Our method achieves the highest recovery success rate and the best image quality.

D. Occlusion Robustness

We consider the de-identification process in special cases, such as face occlusion. As shown in Fig. 9, our approach consistently achieves excellent anonymization results despite facial occlusions. RiDDLE [7] relies on the face parsing model [36] to complete the task of background preservation, which results in separation between the background and the occluded parts, making the results lack naturalness. FIT [5] effectively anonymizes the identity of the face. However, the quality of the generated image is poor and significantly different from the original image. DeepPrivacy [2] and CIAGAN [3] still cannot solve the occlusion task, resulting in artifacts. Our method successfully achieves de-identification while preserving occlusions, producing realistic and smooth results.

E. Diversity of Identities

Fig. 10 shows our diverse anonymization results. As can be seen, our de-identified faces are significantly different in the eyes and mouth. At the same time, the details of the face are more prosperous, and the connection between the background and the face is smoother than other methods. Fig. 11 shows the experimental results of diversity achieved through different anonymity methods. FIT [5] tends to generate similar facial features, which makes the generated anonymous results similar. RiDDLE [7] has diverse identities, but there is a sense of separation between the face and the scene. The result lacks realistic facial details, such as the face’s lighting and the skin’s

texture. Our de-identification method generates realistic and smooth anonymous faces while maintaining identity diversity.



Fig. 10. Diverse anonymization results on the FFHQ test dataset. The first column is the original images and the rest are anonymized images generated using different passwords.

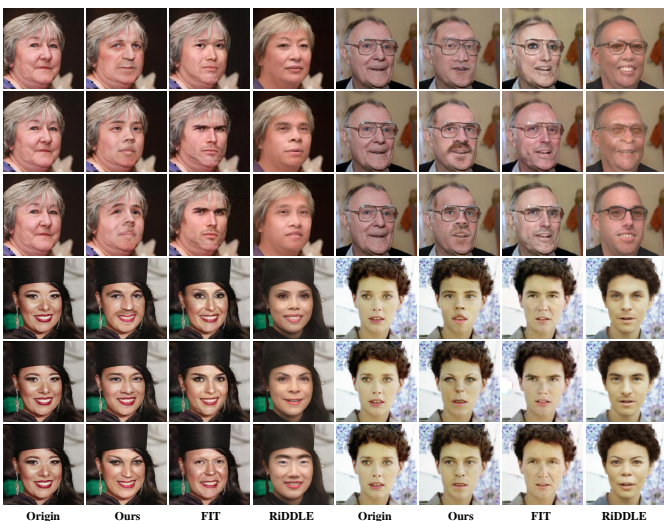


Fig. 11. Comparison of diversity with existing methods. The left is from the FFHQ test set, and the right is from the CelebA-HQ dataset.

To further demonstrate diversity, we conducted visualization experiments. We conduct visualization experiments using identity features to assess identity differences between anonymous faces visually. We only compare with de-identification methods using passwords and reversibility. Five randomly selected face images on the CelebA-HQ dataset were anonymized using 200 passwords for each method. Then, we extracted face identity embeddings using ArcFace [33], FaceNet (VGGFace2), and FaceNet (CASIA), respectively, and reduced the dimensionality of the identity features using t-SNE. Fig. 12 shows the visualization results. If the identities are consistent, they will overlap, and their identity points will take up less space. Our method and RiDDLE [7] occupy a larger space in the hyperplane and outperform FIT [5] on multiple face recognition models. In the results of ArcFace, our method is more dispersed than RiDDLE [7]. The results of FaceNet

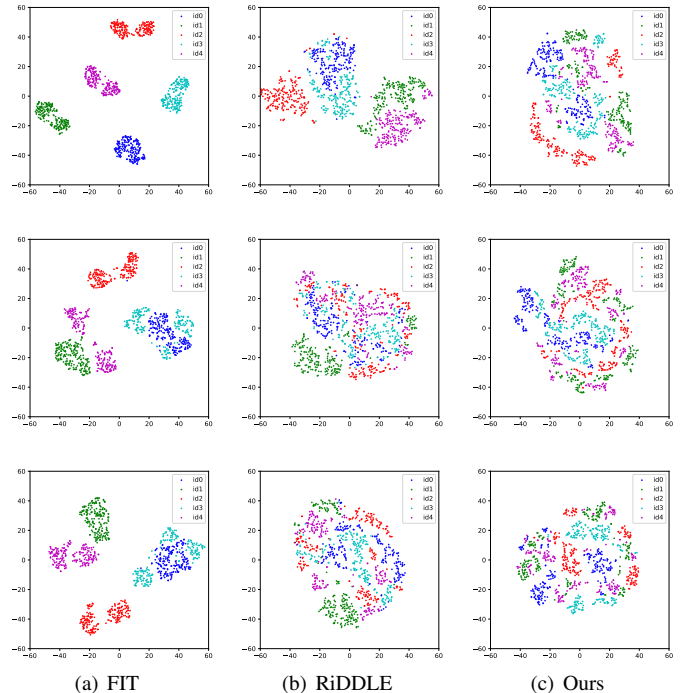


Fig. 12. Visualization results of anonymous diversity. The larger the space occupied by an identity point, the richer the identity. The first row represents ArcFace [33] extracting identity features. The second row represents FaceNet (VGGFace2) that extracts identity features. The third row represents FaceNet (CASIA) extracting identity features.

(VGGFace2) and FaceNet (CASIA) extracted face identity embeddings make it easier to observe that our points with the same identity before anonymity are more dispersed than RiDDLE’s. This phenomenon demonstrates not only the diversity of our approach but also the significant differences between anonymous identities.

TABLE III
UTILITY EVALUATION OF ANONYMOUS IMAGES, WHERE THE VALUES IN THE FIRST, SECOND, AND THIRD COLUMNS REPRESENT THE MEASUREMENTS ON MTCNN [40] AND DLIB [41], RESPECTIVELY. THE LEFT SIDE OF THE SLASH IS MTCNN, AND THE RIGHT SIDE IS DLIB. THE BEST RESULTS ARE SHOWN IN **BOLD**, AND THE SECOND BEST RESULTS ARE MARKED WITH AN UNDERLINE.

Method	Face detection \uparrow	Bounding box distance \downarrow	Landmark distance \downarrow	FID \downarrow
CIAGAN [3]	0.997/0.953	22.605/20.091	8.844/11.874	88.831
FIT [5]	1.000/0.993	5.663/4.489	2.379/2.639	24.578
RiDDLE [7]	1.000/1.000	6.164/5.201	3.619/3.658	29.973
DeepPrivacy [2]	1.000/0.993	6.131/ <u>4.351</u>	4.353/4.116	28.652
Ours	1.000/1.000	4.972/3.905	<u>2.540/3.006</u>	9.610

F. Image Utility

Table III shows the quantitative results. RiDDLE [7] and our method achieve the highest face detection success rate. In addition, we also calculate the pixel-level distance between the anonymized image and the original image to evaluate the degree of facial information preservation. As shown in Table III, our average pixel difference from the original face is relatively low, so our method can better preserve the overall facial information. We also measure the quality of anonymized

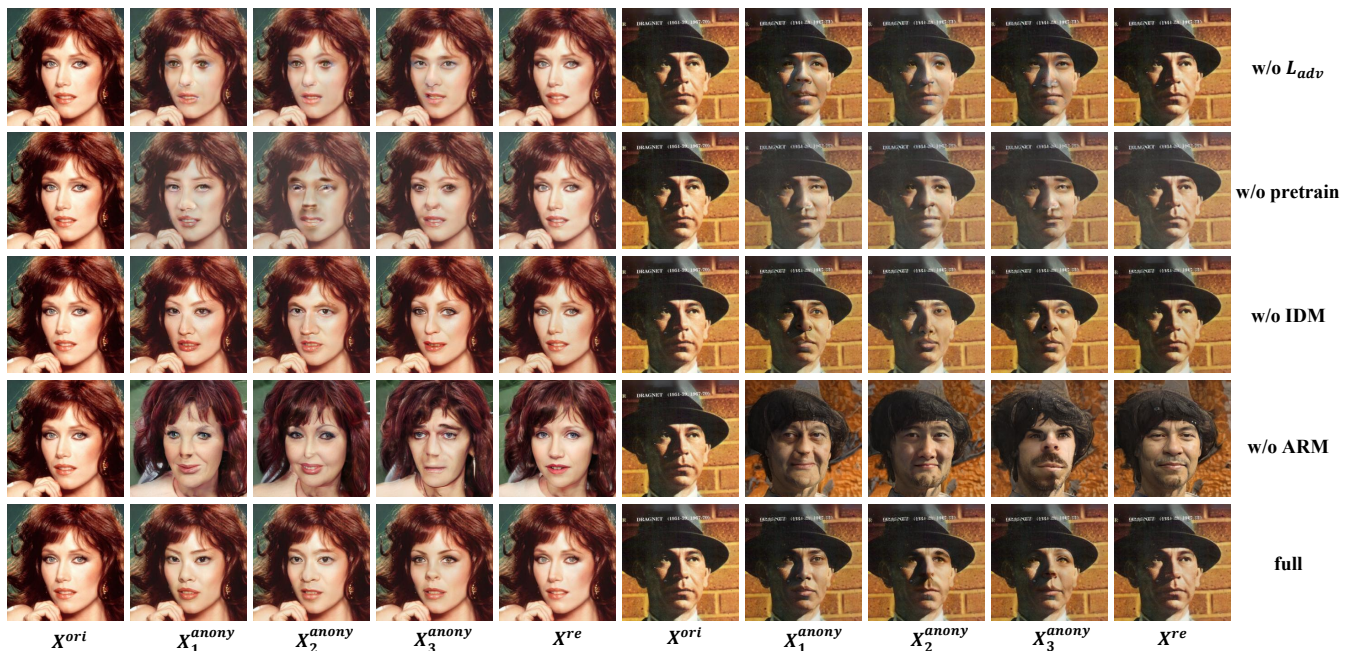


Fig. 13. Qualitative ablation results for key modules and strategies. The above figure shows the anonymization and recovery results for different ablation scenarios.

images by measuring the Fréchet Inception Distance (FID). Our method achieves the lowest FID, indicating that our de-identification has the best generation quality compared to existing methods.

G. Ablation Study

Finally, we evaluate the contribution of important components and training strategies in the model. *w/o L_{adv}* represents training without an adversarial loss. *w/o pretrain* means not pre-trained with additional policies. *w/o ARM* represents that the network removes ARM. *w/o IDM* represents replacing the IDM with a simple disentanglement module consisting of 4 layers of MLP. Fig. 13 shows the results of the qualitative experiments, and Table IV shows the results of the quantitative experiments. From the experimental results, it is clear that adversarial loss can increase the naturalness of anonymous faces. Without adversarial losses, unnatural artifacts appear on the face. Due to the complexity of the loss in the anonymization phase, combining image quality and anonymity is only possible when the network adopts a pre-trained model obtained through a supplementary strategy. The IDM facilitates identity changes and protects attribute details. The ARM is used to generate anonymous images with consistent backgrounds.

V. CONCLUSION

This work proposes a novel privacy-preserving framework HFORD that enables high-fidelity and occlusion-robust de-identification in GAN inversion space. Benefiting from the proposed IDM, our method shows better results in disentangling identities and attributes. This module enhances the network’s face de-identification capabilities while retaining details irrelevant to identity. With the proposed ARM, our

TABLE IV
QUANTITATIVE ABLATION RESULTS. MEASURED FROM PRIVACY PROTECTION, RECOVERY RESULTS, AND IMAGE QUALITY. THE BEST RESULTS ARE SHOWN IN **BOLD**, AND THE SECOND BEST RESULTS ARE MARKED WITH AN UNDERLINE.

	De-id.↓	Recovery↑	FID↓
<i>w/o L_{adv}</i>	0.070	1.000	14.298
<i>w/o pretrain</i>	0.030	1.000	16.375
<i>w/o IDM</i>	<u>0.035</u>	<u>0.990</u>	<u>11.070</u>
<i>w/o ARM</i>	0.035	0.965	39.411
full	0.030	1.000	9.610

approach is more robust to challenging situations, such as images with occlusions, and generates results with higher fidelity. In the future, we will consider face de-identification in various unique situations (e.g., low light, large poses) to make the method more generalizable.

REFERENCES

- [1] N. Vishwamitra, B. Knijnenburg, H. Hu, Y. P. Kelly Caine *et al.*, “Blur vs. block: Investigating the effectiveness of privacy-enhancing obfuscation for images,” in *Proceedings of the IEEE Conference on Computer Vision and Pattern Recognition Workshops*, 2017, pp. 39–47.
- [2] H. Hukkelås, R. Mester, and F. Lindseth, “Deepprivacy: A generative adversarial network for face anonymization,” in *Advances in Visual Computing: 14th International Symposium on Visual Computing, ISVC 2019, Lake Tahoe, NV, USA, October 7–9, 2019, Proceedings, Part I 14*. Springer, 2019, pp. 565–578.
- [3] M. Maximov, I. Elezi, and L. Leal-Taixé, “Ciagan: Conditional identity anonymization generative adversarial networks,” in *Proceedings of the IEEE/CVF conference on computer vision and pattern recognition*, 2020, pp. 5447–5456.
- [4] O. Gafni, L. Wolf, and Y. Taigman, “Live face de-identification in video,” in *Proceedings of the IEEE/CVF International Conference on Computer Vision*, 2019, pp. 9378–9387.
- [5] X. Gu, W. Luo, M. S. Ryoo, and Y. J. Lee, “Password-conditioned anonymization and deanonymization with face identity transformers,” in *Computer Vision–ECCV 2020: 16th European Conference, Glasgow,*

- UK, August 23–28, 2020, *Proceedings, Part XXIII 16*. Springer, 2020, pp. 727–743.
- [6] J. Cao, B. Liu, Y. Wen, R. Xie, and L. Song, “Personalized and invertible face de-identification by disentangled identity information manipulation,” in *Proceedings of the IEEE/CVF International Conference on Computer Vision*, 2021, pp. 3334–3342.
- [7] D. Li, W. Wang, K. Zhao, J. Dong, and T. Tan, “Riddle: Reversible and diversified de-identification with latent encryptor,” in *Proceedings of the IEEE/CVF Conference on Computer Vision and Pattern Recognition*, 2023, pp. 8093–8102.
- [8] T. Karras, S. Laine, and T. Aila, “A style-based generator architecture for generative adversarial networks,” in *Proceedings of the IEEE/CVF conference on computer vision and pattern recognition*, 2019, pp. 4401–4410.
- [9] T. Karras, S. Laine, M. Aittala, J. Hellsten, J. Lehtinen, and T. Aila, “Analyzing and improving the image quality of stylegan,” in *Proceedings of the IEEE/CVF conference on computer vision and pattern recognition*, 2020, pp. 8110–8119.
- [10] Y. Wu, F. Yang, and H. Ling, “Privacy-protective-gan for face de-identification,” *arXiv preprint arXiv:1806.08906*, 2018.
- [11] S. Barattin, C. Tzelepis, I. Patras, and N. Sebe, “Attribute-preserving face dataset anonymization via latent code optimization,” in *Proceedings of the IEEE/CVF Conference on Computer Vision and Pattern Recognition*, 2023, pp. 8001–8010.
- [12] Z. Ren, Y. J. Lee, and M. S. Ryoo, “Learning to anonymize faces for privacy preserving action detection,” in *Proceedings of the european conference on computer vision (ECCV)*, 2018, pp. 620–636.
- [13] Q. Sun, L. Ma, S. J. Oh, L. Van Gool, B. Schiele, and M. Fritz, “Natural and effective obfuscation by head inpainting,” in *Proceedings of the IEEE Conference on Computer Vision and Pattern Recognition*, 2018, pp. 5050–5059.
- [14] Q. Sun, A. Tewari, W. Xu, M. Fritz, C. Theobalt, and B. Schiele, “A hybrid model for identity obfuscation by face replacement,” in *Proceedings of the European conference on computer vision (ECCV)*, 2018, pp. 553–569.
- [15] J. Bao, D. Chen, F. Wen, H. Li, and G. Hua, “Towards open-set identity preserving face synthesis,” in *Proceedings of the IEEE conference on computer vision and pattern recognition*, 2018, pp. 6713–6722.
- [16] J. Li, L. Han, R. Chen, H. Zhang, B. Han, L. Wang, and X. Cao, “Identity-preserving face anonymization via adaptively facial attributes obfuscation,” in *Proceedings of the 29th ACM International Conference on Multimedia*, 2021, pp. 3891–3899.
- [17] Y. Nitzan, A. Bermano, Y. Li, and D. Cohen-Or, “Face identity disentanglement via latent space mapping,” *arXiv preprint arXiv:2005.07728*, 2020.
- [18] Y. Luo, J. Zhu, K. He, W. Chu, Y. Tai, C. Wang, and J. Yan, “Styleface: Towards identity-disentangled face generation on megapixels,” in *Computer Vision–ECCV 2022: 17th European Conference, Tel Aviv, Israel, October 23–27, 2022, Proceedings, Part XVI*. Springer, 2022, pp. 297–312.
- [19] S. Na, “Mfim: Megapixel facial identity manipulation,” in *Computer Vision–ECCV 2022: 17th European Conference, Tel Aviv, Israel, October 23–27, 2022, Proceedings, Part XIII*. Springer, 2022, pp. 143–159.
- [20] Y. Shen, P. Luo, J. Yan, X. Wang, and X. Tang, “Faceid-gan: Learning a symmetry three-player gan for identity-preserving face synthesis,” in *Proceedings of the IEEE conference on computer vision and pattern recognition*, 2018, pp. 821–830.
- [21] A. Shoshan, N. Bhonker, I. Kviatkovsky, and G. Medioni, “Gan-control: Explicitly controllable gans,” in *Proceedings of the IEEE/CVF international conference on computer vision*, 2021, pp. 14083–14093.
- [22] T. Ma, D. Li, W. Wang, and J. Dong, “Cfa-net: Controllable face anonymization network with identity representation manipulation,” *arXiv preprint arXiv:2105.11137*, 2021.
- [23] M.-H. Le and N. Carlsson, “Styleid: Identity disentanglement for anonymizing faces,” *arXiv preprint arXiv:2212.13791*, 2022.
- [24] Y. Jeong, J. Choi, S. Kim, Y. Ro, T.-H. Oh, D. Kim, H. Ha, and S. Yoon, “Ficgan: facial identity controllable gan for de-identification,” *arXiv preprint arXiv:2110.00740*, 2021.
- [25] R. Abdal, Y. Qin, and P. Wonka, “Image2stylegan: How to embed images into the stylegan latent space?” in *Proceedings of the IEEE/CVF International Conference on Computer Vision*, 2019, pp. 4432–4441.
- [26] —, “Image2stylegan++: How to edit the embedded images?” in *Proceedings of the IEEE/CVF conference on computer vision and pattern recognition*, 2020, pp. 8296–8305.
- [27] J. Zhu, Y. Shen, D. Zhao, and B. Zhou, “In-domain gan inversion for real image editing,” in *Computer Vision–ECCV 2020: 16th European Conference, Glasgow, UK, August 23–28, 2020, Proceedings, Part XVII 16*. Springer, 2020, pp. 592–608.
- [28] Y. Alaluf, O. Patashnik, and D. Cohen-Or, “Restyle: A residual-based stylegan encoder via iterative refinement,” in *Proceedings of the IEEE/CVF International Conference on Computer Vision*, 2021, pp. 6711–6720.
- [29] E. Richardson, Y. Alaluf, O. Patashnik, Y. Nitzan, Y. Azar, S. Shapiro, and D. Cohen-Or, “Encoding in style: a stylegan encoder for image-to-image translation,” in *Proceedings of the IEEE/CVF conference on computer vision and pattern recognition*, 2021, pp. 2287–2296.
- [30] O. Tov, Y. Alaluf, Y. Nitzan, O. Patashnik, and D. Cohen-Or, “Designing an encoder for stylegan image manipulation,” *ACM Transactions on Graphics (TOG)*, vol. 40, no. 4, pp. 1–14, 2021.
- [31] A. Dosovitskiy, L. Beyer, A. Kolesnikov, D. Weissenborn, X. Zhai, T. Unterthiner, M. Dehghani, M. Minderer, G. Heigold, S. Gelly *et al.*, “An image is worth 16x16 words: Transformers for image recognition at scale,” *arXiv preprint arXiv:2010.11929*, 2020.
- [32] A. Vaswani, N. Shazeer, N. Parmar, J. Uszkoreit, L. Jones, A. N. Gomez, Ł. Kaiser, and I. Polosukhin, “Attention is all you need,” *Advances in neural information processing systems*, vol. 30, 2017.
- [33] J. Deng, J. Guo, N. Xue, and S. Zafeiriou, “Arcface: Additive angular margin loss for deep face recognition,” in *Proceedings of the IEEE/CVF conference on computer vision and pattern recognition*, 2019, pp. 4690–4699.
- [34] R. Zhang, P. Isola, A. A. Efros, E. Shechtman, and O. Wang, “The unreasonable effectiveness of deep features as a perceptual metric,” in *Proceedings of the IEEE conference on computer vision and pattern recognition*, 2018, pp. 586–595.
- [35] T. Karras, T. Aila, S. Laine, and J. Lehtinen, “Progressive growing of gans for improved quality, stability, and variation,” *arXiv preprint arXiv:1710.10196*, 2017.
- [36] C.-H. Lee, Z. Liu, L. Wu, and P. Luo, “Maskgan: Towards diverse and interactive facial image manipulation,” in *Proceedings of the IEEE/CVF Conference on Computer Vision and Pattern Recognition*, 2020, pp. 5549–5558.
- [37] L. Mescheder, A. Geiger, and S. Nowozin, “Which training methods for gans do actually converge?” in *International conference on machine learning*. PMLR, 2018, pp. 3481–3490.
- [38] F. Schroff, D. Kalenichenko, and J. Philbin, “Facenet: A unified embedding for face recognition and clustering,” in *2015 IEEE Conference on Computer Vision and Pattern Recognition (CVPR)*, 2015, pp. 815–823.
- [39] X. He, M. Zhu, D. Chen, N. Wang, and X. Gao, “Diff-privacy: Diffusion-based face privacy protection,” *arXiv preprint arXiv:2309.05330*, 2023.
- [40] K. Zhang, Z. Zhang, Z. Li, and Y. Qiao, “Joint face detection and alignment using multitask cascaded convolutional networks,” *IEEE signal processing letters*, vol. 23, no. 10, pp. 1499–1503, 2016.
- [41] V. Kazemi and J. Sullivan, “One millisecond face alignment with an ensemble of regression trees,” in *Proceedings of the IEEE conference on computer vision and pattern recognition*, 2014, pp. 1867–1874.